



Spin-resonant suppression and enhancement in ZnSe/Zn_{1-x}MnxSe multilayer heterostructures

著者	Guo Yong, Gu Bing-Lin, Wang Hao, Kawazoe Yoshiyuki
journal or publication title	Physical Review. B
volume	63
number	21
page range	214415
year	2001
URL	http://hdl.handle.net/10097/53381

doi: 10.1103/PhysRevB.63.214415

Spin-resonant suppression and enhancement in $\text{ZnSe}/\text{Zn}_{1-x}\text{Mn}_x\text{Se}$ multilayer heterostructures

Yong Guo

*Department of Physics, Tsinghua University, Beijing 100084, People's Republic of China
and Institute for Materials Research, Tohoku University, Sendai 980-8577, Japan*

Bing-Lin Gu and Hao Wang

Department of Physics, Tsinghua University, Beijing 100084, People's Republic of China

Yoshiyuki Kawazoe

Institute for Materials Research, Tohoku University, Sendai 980-8577, Japan

(Received 6 February 2001; published 10 May 2001)

We investigate spin-polarized transport through semimagnetic semiconductor heterostructures under the influence of both an external electric field and a magnetic field. The structural symmetric and asymmetric effects as well as the electric-field effect are stressed. The results indicate that (1) transmission resonances are drastically suppressed for spin electrons tunneling through the symmetric heterostructure under an applied bias; and (2) transmission resonances can be enhanced to optimal resonances for spin-up electrons tunneling through the asymmetric structure with double paramagnetic layers under a certain *positive bias*, while for spin-down ones tunneling through the same structure, resonances can also be enhanced to optimal resonances under a certain *negative bias*. Transmission suppression and enhancement originate from magnetic- and electric-field-induced and structure-tuned potentials. Spin-dependent resonant enhancement and negative differential resistances can be clearly seen in the current density. The results shown in this work might shed light on design and applications of spintronic devices.

DOI: 10.1103/PhysRevB.63.214415

PACS number(s): 75.50.Pp, 72.10.-d, 84.32.-y

I. INTRODUCTION

Recently the nascent field of “spintronics” has attracted considerable attention,^{1–22} fueled by the possibility of producing efficient photoemitters with a high degree of polarization of the electron beam, creating spin-memory devices¹ and spin transistors² as well as exploiting the properties of spin coherence for quantum computation.³ Most of the proposed spintronic devices involve spin-polarized transport across interfaces in various hybrid structures. To determine the feasibility of spintronic devices and more generally of various applications of spin-polarized transport, it is essential to answer questions like how to create and detect spin-polarized carriers and how to maintain their spin polarization and spin coherence for a relatively long time.

There has been great theoretical and experimental progress made in spin transport through semimagnetic semiconductor systems. Mn- or Fe-based spin superlattices were proposed by von Ortenberg⁷ and realized by Dai *et al.*⁸ and Chou *et al.*⁹ Sugakov and Yatskevich¹⁰ examined spin splitting in parallel electric and magnetic fields through a double-barrier heterojunction using a transfer-matrix method. Recently, Carlos Egues¹¹ investigated spin filtering in a $\text{ZnSe}/\text{Zn}_{1-x}\text{Mn}_x\text{Se}$ heterostructure with a single paramagnetic layer and found a strong suppression of the spin-up component of the current density for increasing magnetic fields. Later, it was further shown that an applied electric field can greatly change the status of the spin polarization of tunneling electrons through a semimagnetic semiconductor heterostructure with a single paramagnetic layer.¹² Very recently, several groups have successfully passed spin-polarized current into a GaAs-based light-emitting diode with high efficiency by use of a semiconductor doped with

Mn. Fiederling *et al.*¹³ used the magnetic semiconductor ZnSe doped with Be and Mn as the spin-aligning ferromagnetic layer. Ohno *et al.*¹⁴ used Mn-doped GaAs. Jonker and his coworkers^{15,16} have performed similar experiments using paramagnetic ZnMnSe as the spin aligner and observed about 50% optical polarization. Moreover, a model for the ferromagnetism of GaMnAs was developed and the Curie temperatures for other Mn-doped semiconductors were predicted.¹⁷

The aim of this paper is to explore spin-resonant suppression and enhancement in $\text{ZnSe}/\text{Zn}_{1-x}\text{Mn}_x\text{Se}$ heterostructures with double paramagnetic layers. We stress structural symmetry and asymmetry of the system as well as external field effects. The results indicate that there not only exists interesting field-induced and structure-tuned spin-dependent tunneling resonances but also a high degree of polarization of electron beams can be obtained by means of electrons tunneling through multilayers.

II. METHOD

We consider a conduction electron through a $\text{ZnSe}/\text{Zn}_{1-x}\text{Mn}_x\text{Se}$ heterostructure with double paramagnetic layers (see Fig. 1), where electrons interact with the three-dimensional electrons of the localized magnetic moments of the Mn ions via the *sp-d* exchange interaction, that can be described as a Heisenberg-type Hamiltonian $H_{int} = -\sum_i J(\vec{r} - \vec{R}_i) \vec{S} \cdot \vec{S}_i$. Here \vec{r} and \vec{S} are, respectively, the position and spin of the conduction electron, and i numbers Mn^{2+} ions of positions R_i and spins S_i . Within mean field and for a magnetic field along the z axis, the *sp-d* exchange interaction gives rise to a spin-dependent potential $V_{\sigma_z} = -N_0 \alpha \sigma_z \langle S_z \rangle [\Theta(z) \Theta(L_1 - z) + \Theta(z - L_1 - L_2) \Theta(L_1$

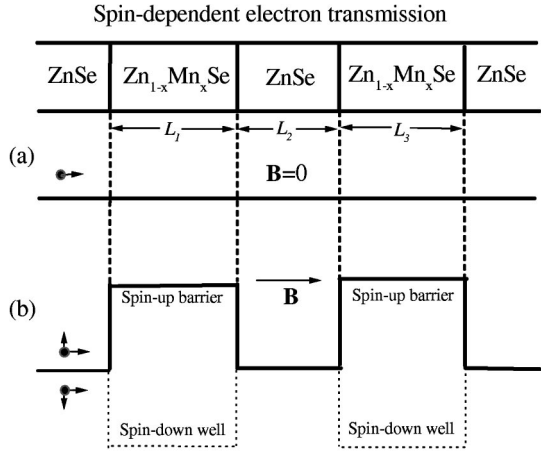


FIG. 1. ZnSe/Zn_{1-x}Mn_xSe multilayers and their conduction-band profile. (a) Zero band offsets potential in the absence of a magnetic field; (b) spin-up electrons see a double-barrier potential while spin-down electrons see a double-well potential under an applied magnetic field.

$+L_2+L_3-z]$ in the Hamiltonian of the system. Here, N_0 is the number of unit cells per unit volume, $\alpha = \langle \Psi | J | \Psi \rangle$ is the exchange integral parameter of the interaction of electrons with Mn²⁺ ions, σ_z are the electron-spin components $\pm 1/2$ along the field, x is the mole fraction of Mn, $\langle S_z \rangle$ is the thermal average of the z th component of a Mn²⁺ spin (a $\frac{5}{2}$ Brillouin function), $\Theta(z)$ is the Heaviside function, L_1 and L_3 are the widths of double paramagnetic layers, and L_2 is the width of the middle ZnSe layer. Under an applied bias V_a along the z axis, an electric-field-induced term $-eV_a z/L_t$ ($L_t = L_1 + L_2 + L_3$) should be added to the potential. In the absence of any kind of electron scattering the motion along the z axis is decoupled from that of the $x-y$ plane. The in-plane motion is quantized in Landau levels with energies $E_n = (n + 1/2)\hbar\omega_c$, where $n = 0, 1, 2, \dots$ and $\omega_c = eB/m_e^*$ (we assume a single electron mass m_e^* throughout the heterostructure). Therefore, the motion of the electrons can be reduced to a one-dimensional problem along the z axis, that can be modeled by the following Hamiltonian within the tight-binding formalism

$$H_z = \sum_{i\sigma_z} (\varepsilon_{i\sigma_z} + U_H \delta n_i) \alpha_{i\sigma_z}^\dagger \alpha_{i\sigma_z} - \sum_{ii'\sigma_z} V \alpha_{i\sigma_z}^\dagger \alpha_{i'\sigma_z}, \quad (1)$$

where the sum over lattice sites i and i' is restricted to nearest neighbors, $V = \hbar^2/2m_e^*a^2$ is the hopping integral and its value is set to one as the energy unit. The Hubbard term $U_H \delta n_i$ ($U_H = 2V$) is added for the self-consistent treatment of charge transfer at the junction, and δn_i is the change in the occupation number at site i , compared to that of the bulk crystal.

The transmission coefficients through the system can be obtained by use of the real-space Green's function and temperature Kubo formula²³ as

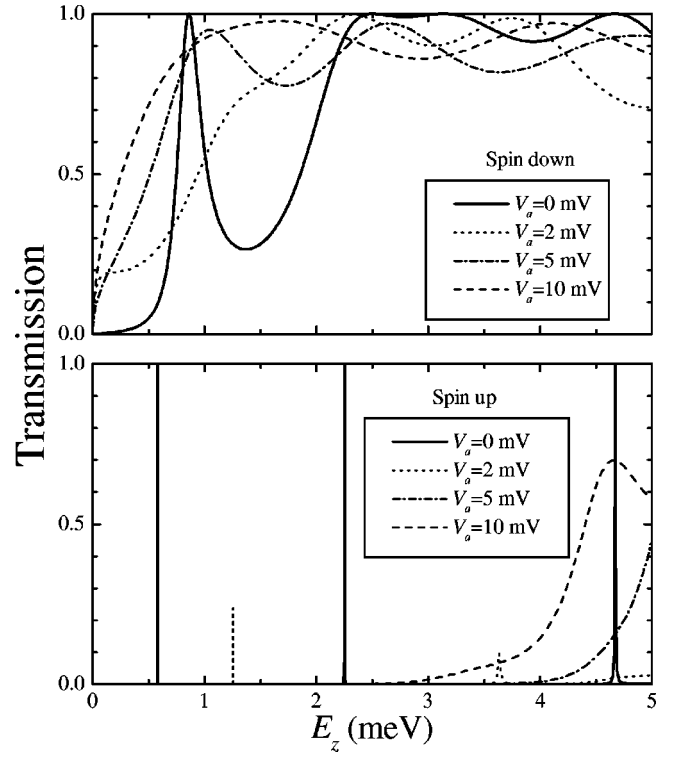


FIG. 2. Spin-dependent transmission coefficients for electrons traversing ZnSe/Zn_{1-x}Mn_xSe multilayers under applied biases. The two paramagnetic layers have the same widths $L_1 = L_3 = 50$ nm. $L_2 = 50$ nm, $B = 2$ T.

$$T_{\sigma_z}(E_z, B, V_a) = \frac{2a^2}{L_z^2} \text{Tr} [\tilde{G}_{\sigma_z}(j, j') \tilde{G}_{\sigma_z}(j' - 1, j - 1) + \tilde{G}_{\sigma_z}(j - 1, j' - 1) \tilde{G}_{\sigma_z}(j', j) - \tilde{G}_{\sigma_z}(j, j' - 1) \tilde{G}_{\sigma_z}(j', j - 1) - \tilde{G}_{\sigma_z}(j - 1, j') \tilde{G}_{\sigma_z}(j' - 1, j)], \quad (2)$$

where $\tilde{G}_{\sigma_z}(j, j') = [G_{\sigma_z}(E_z + i\varepsilon; j, j') + G_{\sigma_z}(E_z - i\varepsilon; j, j')]/2i$ with G_{σ_z} as the matrix element of the real-space Green's function. Note that the transmission coefficients are functions of the incident energy E_z , the magnetic field B , and the applied bias V_a . The spin-dependent density of states (DOS) is related to the Green's function of a whole system via a standard formula $\rho_{\sigma_z}(E_z, B, V_a) = -1/\pi \lim_{\varepsilon \rightarrow 0^+} [\text{Im Tr } G_{\sigma_z}(E_z + i\varepsilon)]$.

We assume that the ZnSe layers are emitter and collector attached to external leads. The average spin-dependent current density is defined by

$$I_{\sigma_z}(B, V_a) = e \sum_{n, k_y, k_z \geq 0} v_z(k_z) T_{\sigma_z}(E_z, B, V_a) \times \left\{ f \left[E_z + \left(n + \frac{1}{2} \right) \hbar \omega_c \right] \right\}$$

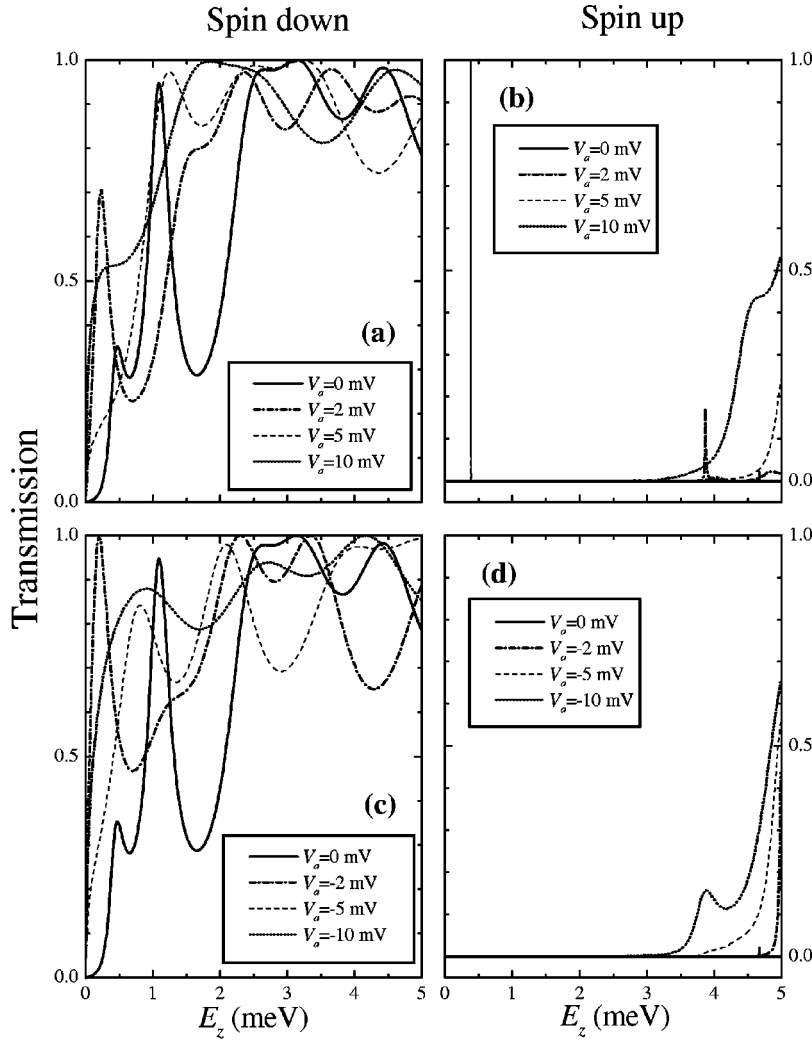


FIG. 3. Spin-dependent transmission coefficients for electrons traversing ZnSe/Zn_{1-x}Mn_xSe multilayers under positive and negative applied biases. The two paramagnetic layers have different widths $L_1=50$, $L_3=100$ nm. $L_2=50$ nm, $B=2$ T.

$$-f\left[E_z + \left(n + \frac{1}{2}\right)\hbar\omega_c + eV_a\right] \times |\psi_{n,k_y,k_z}|^2, \quad (3)$$

where $\psi_{n,k_y,k_z} = (1/\sqrt{L_y})(1/\sqrt{L_z})e^{ik_y y}e^{ik_z z}\varphi_n(x)$. Here, $\varphi_n(x)$ is the n th harmonic-oscillator eigenfunction centered at $x_0 = -\hbar k_y/m\omega_c$, k_y and k_z are the electron wave vectors along the y and z directions. The summation on k_y is equal to $L_x L_y eB/2\pi\hbar$, and $\varphi_n(x)$ is normalized. Therefore, Eq. (3) becomes

$$J_{\sigma_z}(B, V_a) = J_0 B \sum_{n=0}^{\infty} \int_0^{+\infty} T_{\sigma_z}(E_z, B, V_a) \times \left\{ f\left[E_z + \left(n + \frac{1}{2}\right)\hbar\omega_c\right] - f\left[E_z + \left(n + \frac{1}{2}\right)\hbar\omega_c + eV_a\right] \right\} dE_z, \quad (4)$$

where $J_0 = e^2/4\pi^2\hbar^2$.

III. RESULTS AND DISCUSSION

Figure 2 shows the spin-dependent transmission coefficients for an electron traversing a ZnSe/Zn_{1-x}Mn_xSe heterostructure with double identical paramagnetic layers. In all of the graphs, we use $m_e^* = 0.16m_e$, an effective Mn concentration $x_{eff} = x(1-x)^{12}$ with $x=0.05$, $N_0\alpha = 0.26$ eV, and $T = 4.2$ K. At zero bias the magnetic-induced potential is a symmetric double well for spin-down electrons or a symmetric double barrier for spin-up ones, so one can see unit quantum resonances for electrons with different spin orientations. For the spin-up case, we observe three very sharp line-type peaks; within them the transmission is drastically suppressed, which is quite different from that for the spin-down case. In the latter, resonant peaks correspond to above-well virtual-state resonances in electric-well structures. As the applied bias increases, transmission peaks shift to a low-energy region and resonances are drastically suppressed.

Figure 3 presents the transmission coefficients through a ZnSe/Zn_{1-x}Mn_xSe multilayer, where two paramagnetic layers have different widths $L_1=50$ and $L_3=100$ nm. At zero bias, resonances are suppressed, especially for the spin-up case, which reflects typical features for tunneling through asymmetric electric double-barrier or double-well structures.

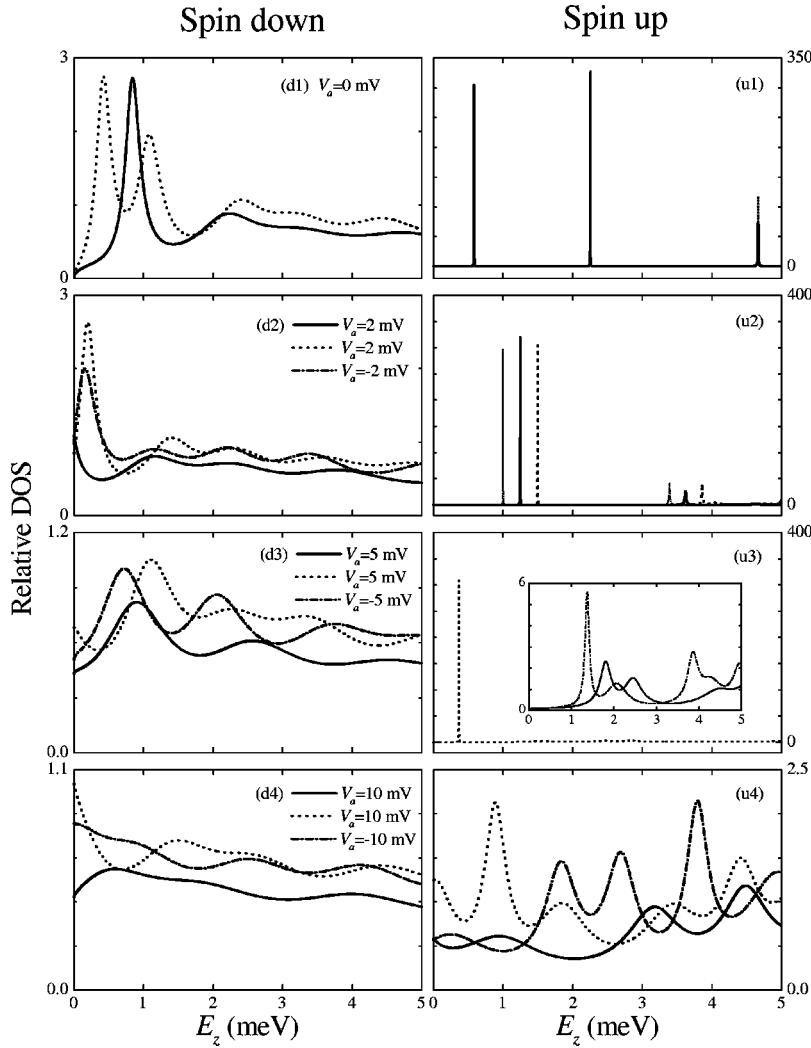


FIG. 4. The relative DOS distribution within symmetric and asymmetric $\text{ZnSe}/\text{Zn}_{1-x}\text{Mn}_x\text{Se}$ systems at zero bias and under applied biases. $L_2 = 50$ nm, $B = 2$ T. Solid line: $L_1 = L_3 = 50$ nm; dotted and dash-dotted lines correspond to the heterostructure with $L_1 = 50$ and $L_3 = 100$ nm under positive and negative biases, respectively.

It is very important to note that the transmission is enhanced to optimal resonances for spin-up electrons tunneling through the asymmetric structure under a certain positive bias [see Fig. 3(b)], while for spin-down ones tunneling through the same structure, the transmission is also enhanced to optimal resonances under a certain negative bias [see Fig. 3(c)]. To the best of our knowledge, we have not seen any discussions on resonant enhancement in well structures. The results obtained here give a solid validity to the similarity of tunneling mechanisms through asymmetric double-well structures and asymmetric double-barrier structures. Note that the magnitude of the effective potential of the system and its symmetry is not only magnetic- and electric-field induced but also structure dependent. In an external magnetic field, the double paramagnetic layers in $\text{ZnSe}/\text{Zn}_{1-x}\text{Mn}_x\text{Se}$ multilayers behave as a double well for spin-down electrons and a double barrier for spin-up ones. As magnetic fields increase, the potential barriers become higher and higher while the potential wells become deeper and deeper, which results in obvious magnetic-field-induced spin polarization in this system. Note also that additional asymmetry can be produced by the external electric field or by the structural asymmetry, thus the spin polarization becomes electric-field induced and structure tuned, which results in interesting

resonant suppression and resonant enhancement.

In order to reveal the nature of structure-tuned and field-induced spin-polarized characteristics, in Fig. 4 we present the relative DOS distribution within the symmetric and asymmetric multilayers. There are a few prominent features summarized here. (1) The distributions of the DOS and its magnitudes for spin-up electrons are drastically different from that for spin-down ones. At zero bias, the DOS is small and the corresponding magnitudes of oscillations are also small for the spin-down case, which correspond to more extended states; for the spin-up case, the DOS shows a sharp line-peak structure with very large peak value, which corresponds to more localized quasibound states. (2) For the symmetric heterostructure, as the electric field increases, the magnitudes of the DOS oscillations monotonously decrease and the corresponding states become more extended. (3) For the asymmetric system, the magnitudes of the DOS oscillations display more complex variations with the intensity and direction of the electric field. The distributions of the DOS show structure-tuned and field-induced features, that correspond to interesting spin-resonant suppression and enhancement. As is well known for electron tunneling through the electric double-barrier structure, when the incident energy of

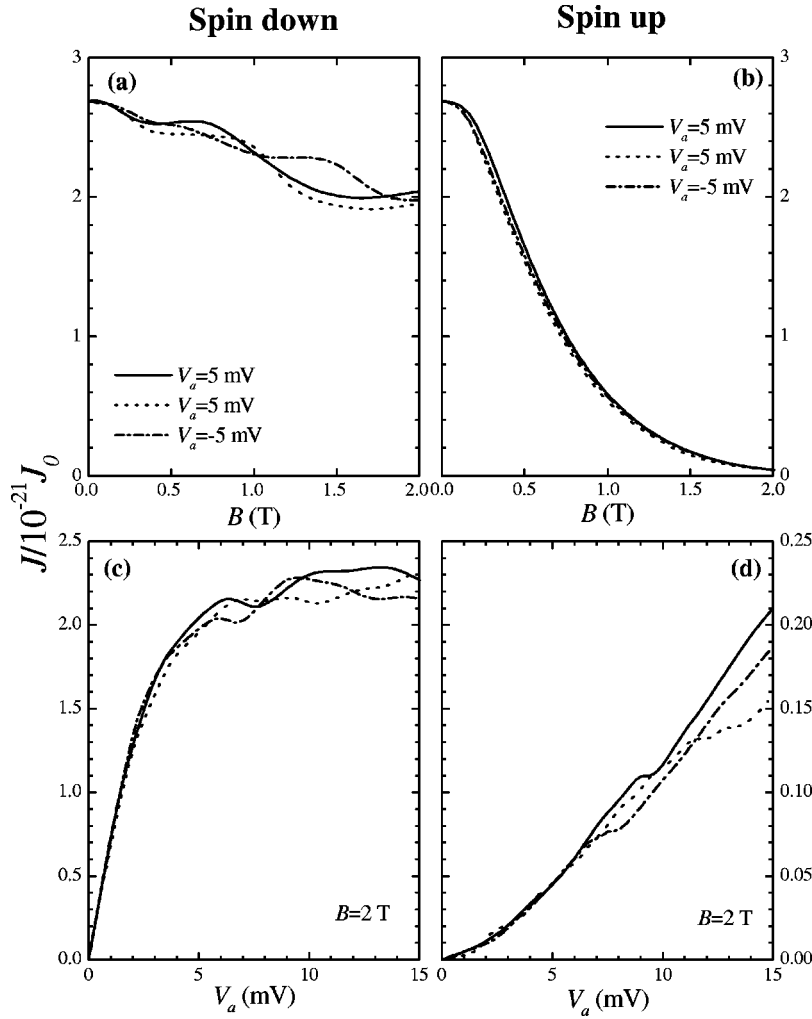


FIG. 5. Spin-dependent current densities for electrons traversing ZnSe/Zn_{1-x}Mn_xSe multilayers. $E_f = 5$ meV. Solid line: $L_1 = L_3 = 50$ nm; dotted and dash-dotted lines correspond to the heterostructure with $L_1 = 50$ and $L_3 = 100$ nm under positive and negative biases, respectively.

electrons coincides with the energy of quasibound states in the potential well, resonant tunneling occurs. This leads to the resonant peaks in the transmission spectrum and oscillations in the DOS spectrum. These quasibound states are localized and the degree of localization is both field induced and structure tuned, which results in the correspondence between the distribution of the DOS and that of the transmission.

Now we examine to what extent the transmission structure is reflected in measurable quantities that involve some kind of average. Figs. 5(a) and (b) show the current density as the function of the magnetic field at a fixed bias, while Figs. 5(c) and (d) show the current density as the function of the bias at a fixed $B = 2$ T. For comparison, we take absolute values of the current density and the bias for the negative bias case. At low bias and low magnetic fields, current densities for spin-up electrons are nearly equal to those for spin-down ones. As the external electric field increases, the current density splits, and the discrepancy between the spin-up case and spin-down cases shows weak oscillations while the global trend is that the difference is first enlarged and then lessened. Further, the larger the magnetic fields, the more obvious is the spin-filtering effect. It is important to note that resonant enhancement can be clearly seen in both the spin-down component and the spin-up component of the current

density [see the dash-dotted line in Fig. 5(c) and the dotted line in Fig. 5(d)] and are due to the spin-dependent resonant enhancement in the transmission coefficient.

IV. CONCLUSIONS

In summary, the effective potential of the semimagnetic semiconductor heterostructure is not only spin dependent but also magnetic- and electric-field induced and structure tuned. The status of spin polarization can be greatly changed by even a small applied bias as well as the structural symmetry. The combined effects result in important spin-resonant suppression and enhancement in the transmission coefficient, which may shed new light on development of spin-dependent microelectronic and optoelectronic devices.

ACKNOWLEDGMENTS

This project was supported by the National Natural Science Foundation of China under Grant No. 10004006 and by the National Key Project of Basic Research Development Plan under Grant No. G2000067107. One of us (Y.G.) gratefully acknowledges the cooperation with the Institute for Materials Research, Tohoku University, Japan.

- ¹J.M. Kikkawa, I.P. Smorchkova, N. Samarth, and D.D. Awschalom, *Science* **277**, 1284 (1997).
- ²D.J. Monsma, R. Vlutters, and J.C. Lodder, *Science* **281**, 407 (1998).
- ³D.P. DiVincenzo, *Science* **270**, 255 (1995); B.E. Kane, *Nature (London)* **393**, 133 (1998).
- ⁴N.N. Kuzma, P. Khandelwal, S.E. Barrett, L.N. Pfeiffer, and K.W. West, *Science* **281**, 686 (1998).
- ⁵G.A. Prinz, *Phys. Today* **48** (4), 58 (1995); *Science* **282**, 1660 (1998).
- ⁶M. Oestreich, *Nature (London)* **402**, 735 (1999).
- ⁷M. von Ortenberg, *Phys. Rev. Lett.* **49**, 1041 (1982).
- ⁸N. Dai, H. Luo, F.C. Zhang, N. Samarth, M. Dobrowolska, and J.K. Furdyna, *Phys. Rev. Lett.* **67**, 3824 (1991).
- ⁹W.C. Chou, A. Petrou, J. Warnock, and B.T. Jonker, *Phys. Rev. Lett.* **67**, 3820 (1991).
- ¹⁰V.I. Sugakov and S.A. Yatskevich, *Sov. Tech. Phys. Lett.* **18**, 134 (1992).
- ¹¹J. Carlos Egues, *Phys. Rev. Lett.* **80**, 4578 (1998).
- ¹²Yong Guo, Hao Wang, Bing-Lin Gu, and Yoshiyuki Kawazoe, *J. Appl. Phys.* **88**, 6614 (2000).
- ¹³R. Fiederling, M. Kein, G. Reuscher, W. Ossau, G. Schmidt, A. Waag, and L.W. Molenkamp, *Nature (London)* **402**, 787 (1999).
- ¹⁴Y. Ohno, D.K. Young, B. Beschoten, F. Matsukura, H. Ohno, and D.D. Awschalom, *Nature (London)* **402**, 790 (1999).
- ¹⁵B.T. Jonker, Y.D. Park, B.R. Bennett, H.-D. Cheong, G. Kioseoglou, and A. Petrou, *Phys. Rev. B* **62**, 8180 (2000).
- ¹⁶R. Fitzgerald, *Phys. Today* **53** (10), 21 (2000).
- ¹⁷T. Dietl, H. Ohno, F. Matsukura, J. Cibert, and D. Ferrand, *Science* **287**, 1019 (2000).
- ¹⁸J.K. Furdyna, *J. Appl. Phys.* **64**, R29 (1988).
- ¹⁹Yong Guo, Bing-Lin Gu, Zhong Zeng, Jing-Zhi Yu, and Yoshiyuki Kawazoe, *Phys. Rev. B* **62**, 2635 (2000).
- ²⁰I.I. Mazin, *Phys. Rev. Lett.* **83**, 1427 (1999).
- ²¹Michael E. Flatté and Jeff M. Byers, *Phys. Rev. Lett.* **84**, 4220 (2000).
- ²²Jürgen König, Hsiu-Hau Lin, and Allan H. MacDonald, *Phys. Rev. Lett.* **84**, 5628 (2000).
- ²³A. Aldea, P. Gartner, and I. Corcotoi, *Phys. Rev. B* **45**, 14 122 (1992).